Raytracing Studies for the Hall D Tagger Dipole using the Tosca Field Maps, and Implications for Field Mapping

Daniel Sober
The Catholic University of America
Version 2 – 14 August 2013

The goals of these studies are

- To test whether the new Tosca field map and the SNAKE raytracing code give results consistent with the rays used in the fixed-array detector layout (Section 3)
- To test whether the proposed field-mapping grid of 1 cm by 2.5 cm is sensible (Section 4)
- To determine how far from the field boundary the fringe field must be measured in order to avoid errors in reconstruction (Section 5)
- To check the differences between the newest version of the SNAKE raytracing code running at JLab (used regularly by the Hall A group) and the "old" version of the code which I am running locally at CUA (Section 6)
- To investigate sensitivity of the ray optics to the incident energy E_0, i.e. the extent to which the position and angle at the focal plane of an electron of given E/E_0 depends on the incident energy E_0, assuming the dipole current is adjusted to give the correct full-energy deflection angle (13.4°) in each case (Section 7)
- To use the results of Sections 4 and 5 to make specific recommendations for field mapping (Section 8)

1. Tosca Field Maps

The field maps were calculated by Yang Guangliang in Glasgow in January 2013, using a coordinate system aligned with the magnet pole edges. (An earlier Tosca field map, used in determining the fixed-array counter layout, was in room coordinates, with the axes at 6.5° to the pole edges.) Maps on a 1 cm × 1 cm grid at 7 different excitations, corresponding to central fields of (approximately) 0.6, 0.9, 1.2, 1.4, 1.5, 1.6 and 1.7 Tesla, are posted at

https://halldweb1.jlab.org/wiki/index.php/Tagger_Magnetic_Field_Maps,

together with the number of ampere-turns used in the calculation. The 1.5 Tesla field is the nominal setting for E_0 = 12 GeV. As expected, the effects of magnetic saturation are small at 1.5 T, but increase rapidly at higher excitations. Figure 1 shows a plot of magnetic field divided by ampere-turns per coil along the line through the center of the magnet pole, transverse to the long exit edge). Except where explicitly stated otherwise in Section 7, I have used only the 1.5 Tesla field map.

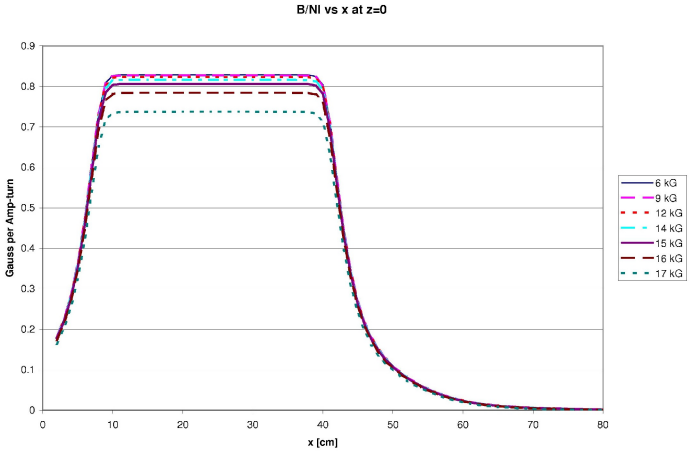

Figure 1.
Comparison of magnetic field per ampere-turn vs transverse coordinate x for all Tosca field maps.

2. Coordinate systems

The origin of the Tosca field map coordinate system is located at the center of the inner long pole edge, at the outer boundary of the flat O-ring surface. (A figure is posted at https://halldweb1.jlab.org/wiki/index.php/Tagger_dipole_tosca_map_coordinates .) The magnet dimensions used in the Tosca calculation are given in Technical Drawing D000001900-1002-REVC (https://halldweb1.jlab.org/wiki/images/f/f3/D000001900-1002-REVC.pdf).

The room coordinate system has its origin at the nominal goniometer position along the beam line. The nominal entry point to the magnet in room coordinates is at (3192.2 mm , 0), and is defined as the intersection of the beam axis with the "pole root" (defined by me as the base of the Rogowski chamfer), 150 mm from the "pole root corner" (defined similarly).

With the dimensions given by the Technical Drawing, the origin of the field map in room coordinates is z = 6319.39 mm, x = -75.46 mm. I initially made a guess for the origin of the field map, and adjusted it to give decent agreement with the rays used in calculating the fixed-array counter layout. Using the final coordinate system described above changed the results only negligibly.

To avoid possible confusion in my use of the symbols x, y, z it should be pointed out that I have had to juggle several different coordinate systems:

Tosca dipole:	z parallel to long dimension, origin at center
	x parallel to short dimension, origin at center of inner pole edge
Somov room:	z along beam line, origin at goniometer
	x to left of beam
SNAKE room:	y along beam line, origin at goniometer
	x to left of beam; z vertical
SNAKE dipole:	SNAKE (x, y) = Tosca (z, x)
Focal plane:	x_{FP} along line at 8.05° to beam axis,
	origin at (-694.0 mm, 4150.9 mm) in room coordinates

3. Comparison with rays used in detector layout

An important first question is how much to trust the initial set of "standard" rays which I used to calculate the fixed-array detector layout. These rays were calculated using the earlier Tosca map, whose unfortunate coordinate system led to considerable spurious structure which had to be smoothed out before I could use the ray data.

To compare the new field map with the "standard" rays, I first adjusted the overall scale of the nominal 1.5 T field by a factor of 0.996772 to give a full-energy deflection of 13.40° for 12 GeV electrons, and then transported a set of on-axis rays through the field. The results are shown in the following table.

Table 1

Comparison of focal plane intercept and in-plane crossing angle for "standard rays" (used in fixed-array layout) and SNAKE calculations using the new 1.5 T Tosca field map with magnetic field scaled for 13.40° bend at 12 GeV. The last column gives the tranvserse position difference, $\Delta x_{transv} = \Delta x_{FP} \sin \theta_x$, which is the difference between the new and old ray intercepts in the plane of the detector face.

Table 1.

	"Standard" rays (2012)		New map (August 2013)		Differences		
E_e (GeV)	x_{FP} (mm)	θ_x (deg)	x_{FP} (mm)	θ_x (deg)	Δx_{FP} (mm)	$\Delta\theta_x$ (deg)	Δx_{transv} (mm)
0.2	-264.34	46.87°	-265.53	46.98°	-1.19	0.11°	-0.87
0.3	0.11	37.94	-1.42	38.03	-1.53	0.09	-0.94
0.5	417.36	29.16	414.84	29.25	-2.52	0.09	-1.23
1	1211.45	20.58	1208.47	20.64	-2.98	0.06	-1.05
2	2436.25	14.74	2432.29	14.78	-3.96	0.04	-1.01
3	3468.86	12.26	3464.78	12.29	-4.08	0.03	-0.87
4	4407.03	10.84	4402.76	10.87	-4.27	0.03	-0.81
5	5286.56	9.91	5282.83	9.93	-3.73	0.02	-0.64
6	6126.70	9.24	6123.17	9.26	-3.53	0.02	-0.57
7	6938.66	8.73	6925.34	8.75	-3.42	0.02	-0.52

Note that the transverse shift is always smaller than a counter width or a Microscope fiber. There are no significant differences from the "standard rays."

4. Dependence of calculations on field map grid size

The initial 1 cm × 1 cm Tosca grid consists of 801 "z" values from -400 to +400 cm and 126 "x" values from -25 to +100 cm. The negative x values are in the coil cavity and return yoke, so I have truncated the map to 101 x values from at x = 0 to 100 cm. I also produced field boxes with alternate points omitted in one or both directions:

1) 1cm by 1cm (801 × 101 points)
2) 1 cm by 2 cm (even z) (801 × 51 points)
3) 1 cm by 2 cm (odd z) (801 × 50 points)
4) 2 cm (even x) by 2 cm (even z) (401 × 51 points)
5) 2 cm (odd x) by 2 cm (even z) (400 × 51 points)
6) 2 cm by 4 cm (401 × 26 points)
7) 4 cm by 2 cm (201 × 51 points)

A standard set of 15 rays starting at the goniometer position

5 electron energies: E_e = 0.3, 1, 2, 3, 4 GeV

For each E_e: on-axis, horizontal angle = $2\theta_{ce}$, vertical angle = $2\theta_{ce}$

where θ_{ce} = electron characteristic angle = $(E_e - E_0)/E_e\,(m_e/E_0)$

was traced through each of these maps. (Only 14 rays survived to the focal plane: the 0.3 GeV ray with vertical angle did not survive the magnet gap.)

Table 2 shows the maximum differences in x_{FP}, θ_x (horizontal angle), z_{FP} (vertical position) and θ_z (vertical angle) between each map and a corresponding map in which the grid differs in only one

direction.

Table 2.

Case	Grid size (cm)	Max. $\lvert \Delta x_{FP} \rvert$ (mm)	Max. $\lvert \Delta\theta_x \rvert$ (deg)	Max. $\lvert \Delta z_{FP} \rvert$ (mm)	Max. $\lvert \Delta\theta_z \rvert$ (deg)
1	1×2 vs 1×1	0.10	0.003	0.02	0.001
2	1×2odd vs 1×1	0.11	0.002	0.04	0.002
3	2×2 vs 1×2	0.09	0.001	0.03	0.001
4	2odd ×2 vs 1×2	0.09	0.001	0.03	0.001
5	2×4 vs 2×2	6.12	0.099	0.12	0.004
6	4×2 vs 2×2	0.35	0.003	0.01	< 0.001

The differences are all negligible except for case 5, in which the field is given in 4 cm steps across the long exit edge, a clearly unreasonable spacing in view of the rapid field variation seen in Figure 1. Note that cases 1 and 2 test the effect of doubling the grid step across the long exit edge, while cases 3 and 4 test doubling the grid step across the entry edge.

My conclusion for field-mapping is that 1 cm steps across the rapidly-changing field boundaries should be more than adequate (but in view of the large variation per cm I would be reluctant to choose a coarser grid.)

5. Effects of the fringe field

A second question for the field mapping is how far we need to extend our measurements into the fringe field region. The Tosca field map at 1.5 Tesla extends to

$z = \pm 400$ cm $\approx$ 89 cm outside the effective field boundary, where B $\approx$ 1 gauss

$x = 100$ cm $\approx$ 57 cm outside the effective field boundary, where B $\approx$ 5 gauss

The effective field boundary (EFB) coincides approximately with the pole root (= base of Rogowski chamfer.)

This field covers most of the focal plane up to nearly $E_e = 5$ GeV, making it possible to trace rays to the focal plane without leaving the field box. It is possible to test the effects of the fringe field in both the entry and exit regions by starting the trajectories at various planes inside the entry field or terminating the raytracing at various planes prior to reaching the focal plane.

Entry fringe field

The fringe field along the entry beam line will have to measured separately from the main field map.

Table 3 shows the effect of ignoring the fringe field outside various distances from the entry EFB. Δx_{FP} and $\Delta\theta_x$ are the differences between the values of x_{FP} and θ_x calculated with the field

cut off at the given distance before the entry EFB and the values calculated using the full Tosca fringe field (starting 89 cm outside the entry EFB). Using on-axis rays only.

Table 3.

Distance outside EFB =	30 cm ($B \approx 58$ gauss)		40 cm ($B \approx 19$ gauss)		50 cm ($B \approx 10$ gauss)		60 cm ($B \approx 6$ gauss)	
E_e (GeV)	Δx_{FP} (mm)	$\Delta\theta_x$ (deg)	Δx_{FP} (mm)	$\Delta\theta_x$ (deg)	Δx_{FP} (mm)	$\Delta\theta_x$ (deg)	Δx_{FP} (mm)	$\Delta\theta_x$ (deg)
0.3	-0.02	0.039	-0.05	0.020	-0.04	0.012	-0.03	0.006
1	0.20	0.008	0.06	0.004	0.02	0.003	0	0.001
2	0.27	0.004	0.11	0.002	0.05	0.001	0.02	0.001
3	0.30	0.002	0.12	0.001	0.06	0.001	0.03	0
4	0.31	0.002	0.12	0.001	0.06	0	0.03	0

The fringe field along the beam line must be measured to at least 40 cm.

Exit fringe field

The focal plane is inclined at 1.55° to the magnet exit edge, and in the region of the magnet its perpendicular distance from the EFB varies from about 43 cm to about 57 cm. We can terminate the raytracing at planes of various distances from the EFB and transport the particles along straight lines to the focal plane, and compare the results with full raytracing to the focal plane.

Table 4 shows the differences Δx_{FP} and $\Delta\theta_x$ between the values of x_{FP} and θ_x calculated with the field cut off at the given distance beyond the exit EFB and the values calculated using the full Tosca fringe field to the focal plane. Using on-axis rays only.

Distance outside EFB =	20 cm ($B \approx 197$ gauss)		30 cm ($B \approx 55$ gauss)		40 cm ($B \approx 20$ gauss)	
E_e (GeV)	Δx_{FP} (mm)	$\Delta\theta_x$ (deg)	Δx_{FP} (mm)	$\Delta\theta_x$ (deg)	Δx_{FP} (mm)	$\Delta\theta_x$ (deg)
0.3	0.97	-0.134	0.12	-0.036	-0.01	-0.005
1	1.74	-0.070	0.26	-0.020	0.01	-0.004
2	2.55	-0.040	0.43	-0.015	0.03	-0.004
3	3.16	-0.038	0.58	-0.012	0.06	-0.004
4	3.65	-0.032	0.70	-0.010	0.09	-0.004

If the measured fine-grid field map extends only to 20 or 30 cm, the missing field must be restored using calculations.

Full-energy fringe field

Since the current in the magnet will be adjusted to send the full-energy electron beam to the dump at a deflection angle of 13.4°, the measured field map must include enough of the fringe field along the exit beam line to allow an accurate calculation of this trajectory. As with the entry fringe field, this field will have to measured separately from the main map.

Scaling the field by a factor 0.995865 (which makes the averagefield in the central region equal to 15000 gauss instead of 15036.29), and using the entire entry fringe field, the dependence on the exit fringe field cutoff is given by

Cutoff distance from EFB	Deflection
0	13.367°
20 cm	13.408°
40 cm	13.411°
70 cm	13.411°

As with the entry region, the fringe field along the exit beam line should be measured to 40 cm.

6. Consistency of new and old SNAKE versions

The latest version of SNAKE is used by the Hall A group at JLab. I have been running an older version at CUA. The new code contains some additional features which we do not need, and has some changes in common blocks and calling arguments.
In my work on the Hall B tagger, I embedded all of the crucial subroutines of the "old" code into a Monte Carlo program which included the geometry of the focal plane detectors. It would be much easier to adapt this code for the Hall D tagger than to start again using the new raytracing subroutines. Thus it is important (to me, at least) to test whether the results of the old and new codes are consistent.

The new and old codes accept identical field maps, and are driven by "directive" and "trajectory" files whose formats have changed only slightly. Thus it is straightforward to run the identical problem on both systems, although the standard output files give results in different forms (e.g. projected angle vs tangent) and must be converted.

Table 5 lists the maximum differences between "new" and "old" snake for the same set of 15 trajectories used in testing the grid size in Section 4:

Grid size (cm)	Max. $\lvert \Delta x_{FP} \rvert$ (mm)	Max. $\lvert \Delta\theta_x \rvert$ (deg)	Max. $\lvert \Delta z_{FP} \rvert$ (mm)	Max. $\lvert \Delta\theta_z \rvert$ (deg)
1×1	0.01	0.003	0.01	< 0.001
1×2	0.01	0.003	0.01	0.001
2×2	0.01	0.003	0.03	0.001
2×4	0.03	0.003	0.04	0.002
4×2	0.01	0.003	0.03	0.001

The differences are entirely negligible. Note that this includes the two cases with ridiculously large 4 cm grid spacings, which should be a good indication of any significant differences in the calculation of partial derivatives of the field.

7. Dependence of ray optics on incident energy

Although the nominal operating energy for Hall D is 12 GeV, we cannot exclude the possibility of running with higher or lower energy. It is important to know to what extent the tagger optics (as a function of E_e/E_0) depends on the incident energy E_0, assuming the dipole current is adjusted to give the correct full-energy deflection angle (13.4°) in each case.

I have done some raytracing through the Tosca field maps at the highest and lowest excitations, always adjusting the incident energy to give exactly the same full-energy deflection as at 12 GeV. Presumably if the results at the two extremes do not differ significantly from the 1.5 T field then there is no reason to calculate the intermediate values.

Table 6 shows the differences, relative to the calculations at 1.5 T (12 GeV), of the in-plane focal plane positions and angles, at electron energies corresponding to the same value of E/E_0 as was used at 1.5 T.

	0.6 Tesla vs 1.5 Tesla		1.7 Tesla vs 1.5 Tesla	
scaled E_0 =	4.79 GeV		13.57 GeV	
E_e at 12 GeV	Δx_{FP} (mm)	$\Delta\theta_x$ (deg)	Δx_{FP} (mm)	$\Delta\theta_x$ (deg)
0.3 GeV	0.20	-0.006	-0.37	0.009
1 GeV	0.21	0.005	0.14	-0.023
2 GeV	0.14	0.007	0.78	-0.023
3 GeV	-0.01	0.006	1.21	-0.022
4 GeV	-0.10	0.006	1.85	-0.020

To put the 1.7 Tesla values in perspective, note that at the ends of the Microscope region, the transverse shifts (compared to the 2mm fiber width) are

"3 GeV" ⇒ 9 GeV photon: 1.21 mm × sin(12.2° deg) = 0.23 mm

"4 GeV" ⇒ 8 GeV photon: 1.85 mm × sin(10.8° deg) = 0.35 mm

which I would say is not a serious problem.

Assuming that the saturation effects of the real magnet are comparable to the "standard steel" used in the Tosca calculations, the excitation effects should be very small. Of course, there is no guarantee that the actual magnet behaves this way, which is why we have to map it.
I propose that after mapping at 1.5 T we try maps at the highest and lowest excitations, and immediately look at the ratio $(B/NI)_2/(B/NI)_1$ versus x and y , and compare with the Tosca predictions to see if there are big differences. If not, then there should be no need for measuring full maps for a full set of excitations.

The following section summarizes the field measurements that are needed for accurate calibration of the tagger focal plane.

8. Requirements for field mapping

As a result of the above ray-tracing exercises using the Tosca field map, I have come up with the following suggestions for the field regions needed to be mapped. Figure 2 indicates the desired rectangular "field boxes" by solid black outlines. For some boxes, as discussed below, it will not be possible to measure the field map directly, but the field can be calculated using a more limited set of measurements.

Since I am still uncertain about the dimensions and the coordinate system, I will refer my boxes to what I call the "field edges." These are probably close (within 5mm) to the "boxed" dimensions given by the projection of the second chamfer on Technical Drawing D00000-19-00-0102, which lead to overall pole dimensions of 16.138" by 245.325", or 40.991 by 623.126 cm. Because I am constantly switching between coordinate systems, I will always refer to the "entry edge", "long edge" and "short exit edge". (Negative distances = toward the uniform field region, positive distances = away from the uniform field region.)

Box 1 – Entry region

In magnet coordinates, this should extend approximately from

(Normal to entry edge)	50 cm outside to -10 cm[(1)] inside	1 cm steps
(Normal to long edge)	-5 cm inside to -20 cm inside	2.5 cm steps

Note (1): or far enough to assure at least 5 cm overlap with Box 2

Because of the vacuum chamber, it will be impossible to measure this box directly. An alternative procedure is to measure the field accurately in 1 cm steps along the incident beam axis, from 50 cm outside to 20 cm[(1)] inside, and construct the necessary box by calculation.

Box 2 – Main field region

(Normal to entry edge)

-5 cm[(2)] inside entry edge to -5 cm[(2)] inside exit edge 2.5 cm steps

(Normal to long edge)

-35 cm[(3)] inside to 35 cm outside 1 cm[(4)] steps

Notes: (2) or as close as possible to vacuum chamber wall

(3) or as close as possible to the back wall. The full-energy trajectory extends to ≈32.5 cm from the exit edge by my estimate.

(4) 1 cm steps are necessary near the exit edge (from -10 cm to 10 cm). Could take coarser steps outside this region.

Box 3 – High-energy exit region

For electron energies above ≈6 GeV, the electron leaves the main field box by crossing the plane of the short exit edge. This is a complicated region, in which there is fringe field variation in two directions.

(Normal to short exit edge)	20 cm inside to 50 cm outside	2.5 cm[(5)] steps
(Normal to long edge)	10 cm outside to 20 cm inside	1 cm[(5)] steps

Note (5): This is the spacing of the main field box, which will have to be used as a basis for calculating this field.

Because of the vacuum box, it will not be possible to measure all of this region directly. Some limited measurements outside the vacuum box will be useful in constraining calculations.

Box 4 – Full-energy exit region

As discussed at the end of Section 5, it is important to have a good calculation of the transport of the full-energy electrons to the beam dump. The required field box is almost a mirror image of Box 1 – not quite, because the exit angle is 6.9° instead of 6.5°.

(Normal to short exit edge)	-10 cm[(1)] inside to 50 cm outside	1 cm steps
(Normal to long edge)	-1 cm inside to -20 cm inside	2.5 cm steps

Note (1): or far enough to assure at least 5 cm overlap with Box 2

As with Box 1, the vacuum chamber will make it impossible to measure this box directly. An alternative procedure is to measure the field accurately in 1 cm steps along the incident beam axis, from -20 cm[(1)] inside to 50 cm outside, and construct the necessary box by calculation.

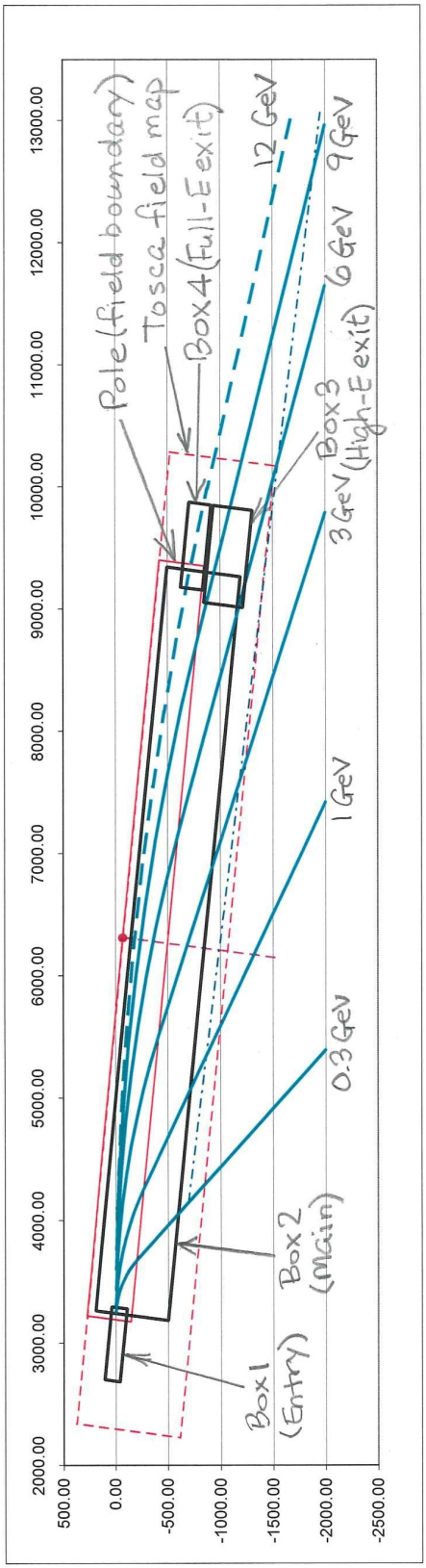

Figure 2.
The solid black lines indicate (approximately) the regions in which the magnetic field must be measured, or calculated using partial measurements, as described in the text.